



Original Paper

Nanoparticles assisted microwave radiation: Fluid-rock interactions in oil reservoirs



Hamzeh Shamsi Armandi, Arezou Jafari*, Reza Gharibshahi

Faculty of Chemical Engineering, Tarbiat Modares University, Tehran, Iran

ARTICLE INFO

Article history:

Received 14 November 2020

Accepted 7 June 2021

Available online 3 September 2021

Edited by Yan-Hua Sun

Keywords:

Microwave radiation
Wettability alteration
Nanoparticle adsorption
Rock-fluid interaction

ABSTRACT

Recently, many researchers have focused on the usage of electromagnetic waves in oil production and well stimulation, but so far the effect of these waves on the fluid and rock interaction and its simultaneous effect with nanoparticles have not been investigated. Fluid-rock interaction is one of the most important factors affecting fluid distribution in the reservoirs. In this study, the oil reservoir rock wettability alteration under electromagnetic heating and the presence of nanoparticles has been investigated. Three nanoparticles of TiO_2 , Fe_3O_4 , and $\text{TiO}_2/\text{Fe}_3\text{O}_4$ have been utilized. TiO_2 nanoparticles are commercially available, and the other mentioned nanoparticles are synthesized via a co-precipitation method. Citric acid has been used to modify surfaces of nanoparticles and stabilize them in water as the base fluid. Also, the adsorption of the nanoparticles on the rock surface has been determined. In the next step, the amount of oil outflow from the rock has been measured and reported as the external fluid imbibition. In this process, the nanoparticle performance in wettability alteration was investigated using pH and inductively coupled plasma (ICP) analyses. To better understand the governing mechanisms, oil viscosity was measured by mixing the oil with nanoparticles and put under irradiation. The results reveal that the microwave has a great ability to reduce oil contact angle with carbonate rock. In the presence of 0.2 wt% Fe_3O_4 nanoparticles, the contact angle was reduced from 155° to 19° after 28 min of irradiation, indicating strong rock hydrophilicity. Furthermore, microwave irradiation on Fe_3O_4 nanofluid extracts 75% of the oil from the rock. With microwave radiation, the pH of the nanofluid increases and hence, more nanoparticles are adsorbed on the rock which subsequently causes more rock dissolution. The viscosity change results prove that there is an optimal irradiation time of 5 min in which oil viscosity reduces from 481 cP to 410 cP and then increases to 827 cP. Moreover, the application of further nanoparticles diminishes the oil viscosity at optimum irradiation time in which Fe_3O_4 has the most oil viscosity reduction, representing 481 cP to 200 cP at 50% microwave power level.

© 2021 The Authors. Publishing services by Elsevier B.V. on behalf of KeAi Communications Co. Ltd. This is an open access article under the CC BY-NC-ND license (<http://creativecommons.org/licenses/by-nc-nd/4.0/>).

1. Introduction

The production of hydrocarbon from heavy oil reservoirs might be challenging due to its high viscosity and low mobility (Speight, 2013). The use of conventional enhanced oil recovery techniques in heavy oil reservoirs including the injections of water, gas, and chemicals may affect the ultimate production. These methods, in comparison with the thermal ones, have lower efficiency due to the strong hydrophobicity of rock, high viscosity difference between the displacing and displaced fluids, and the viscous fingering

phenomenon (Doorwar and Mohanty, 2011; Kadeethum et al., 2017). Lowering the oil viscosity and improving its quality in the reservoir are some of the strategies that can be achieved by thermal methods for heavy oil reservoirs. Each of the thermal methods such as hot water injection, steam injection, steam-assisted gravity drainage (SAGD), and in-situ combustion reduce oil viscosity and cause mobility enhancement, resulting in greater oil production of these reservoirs. However, in the use of high-temperature fluid injection, there is a need to supply a large volume of primary fluid (water) and high energy to increase its temperature. Also, the high temperature of such fluids causes the corrosion of the associated field equipment (Zaydullin, 2013; Zekri et al., 2000). These approached are dependent on the formation depth in a way that at high depths, fluid heat is directed to adjacent formations and is not

* Corresponding author.

E-mail address: ajafari@modares.ac.ir (A. Jafari).

longer capable of raising the reservoir temperature (Tunio et al., 2011). In the oil combustion method, a large volume of oil is combusted in the reservoir, and the combustion front control is not easy (Millemann et al., 1982; Zaydullin, 2013; Zekri et al., 2000; Tunio et al., 2011). Therefore, new approaches are demanded to overcome such challenges. Electromagnetic heating is one of the most novel methods that has overcome most of the mentioned hurdles.

By electromagnetic radiation, the dipole moment is applied to the molecules of the material, and they begin to rotate in alternating orientations along the field. As a result of these orientations, friction is initiated between the molecules, and heat is generated (Bera and Babadagli, 2015). Each material has its own dielectric constant and reacts differently to other materials in the electromagnetic field (Bera and Babadagli, 2015). Having this in mind, it might be concluded that electromagnetic waves have selective heating properties (Anwar et al., 2015). The dielectric constant of oil falls in the ranges of 2–4 (Liao et al., 2018) while this value has been proved to be 80.2 for water (Archer and Wang, 1990). So, compared to the oil phase, water can absorb higher amount of electromagnetic energy and consequently heats up faster and easier. The more absorption of wave energy by water, the more directed energy to farther points of the reservoir.

Another usage of microwave is its impact on oil viscosity. Microwave radiation does not necessarily reduce the oil viscosity under radiation. Shang et al. (2018) have represented that depending on the type of oil and its composition, both increasing or decreasing patterns of viscosity are expected. They pointed out that the changes in viscosity depend on several factors, including the amount of oxygen content and the resin/asphaltene ratio. Taheri Shakib et al. (2017) compared the conventional heating technology (CHT) with electromagnetic heating technology (MHT). It was reported that the sulfur content of the oil decreased during the MHT process, while CHT did not affect the sulfur content. It was also stated that the C–S bond has a high microwave absorption capacity and is also a weak bond. Furthermore, it was mentioned that the weak C–S bond has a high microwave absorption capacity. Chakma et al. (1999) observed that with increasing frequency from 5 to 20 MHz, the production rate enhanced from 29% to 37%, respectively. It was also found that the oil recovery increased by about 13% through gas injecting process under the electromagnetic radiation at a frequency of 10 MHz. Hu et al. (2017) reported that as the microwave power level increased from 0 to 30, the production efficiency improved significantly from 0% to about 58%.

One of the most serious challenges is that due to the absorption of microwaves by formation materials, the penetration depth of the waves within the pay zone is diminished, and thus the heat generated inside the reservoir is difficult to transfer to farther points (Gharibshahi et al., 2020). It must be regarded that the heat needs to be transferred by convection and conduction mechanisms to heat the farther points away from the wellbore. For this purpose, an injection fluid with a high absorption capacity of electromagnetic waves is required. This fluid might be water, some solvents like *n*-hexane, or even nanofluids. Nanoparticles with extraordinary properties such as size, high surface energy, electrical conductivity, and high heat capacity, as well as Brownian motion, have a significant effect on the rock and fluid properties of the reservoir (Al-Farsi et al., 2016). The utilization of nanofluids has attracted a great deal of attention due to their high electromagnetic waves absorption capacity and their promising influence on the wettability alternation, interfacial tension, and oil relative permeability (Bahraminejad et al., 2019). Taheri Shakib et al. (2018c) employed three nanoparticles comprising of super activated carbon (CA), iron powder (Fe), and titanium oxide (TO) to investigate the oil temperature rise and its viscosity change under the influence of

microwave. After 10 min of irradiation, the temperature of the oil containing the CA, Fe, and TO nanoparticles increased from the ambient temperature to 196, 170, and 158 °C, respectively. The viscosity results demonstrated that among all the above-mentioned nanoparticles, CA had the highest effect on reducing this parameter. The oil viscosity of the nanoparticles decreased from 880 cP before irradiation to 791.19 cP after 6 min of irradiation. Greff and Babadagli (2013) proved that following the microwave irradiation, nickel nanoparticles would reduce the viscosity of petroleum more than both iron powder and Fe₃O₄ nanoparticles. Alnarabiji et al. (2018) utilized ZnO nanocrystals distributed in water as an injection fluid at 2 W electromagnetic wave power and a frequency of 13.6 MHz. The results showed a 23.3% increase in oil production compared to the non-irradiated state. It was claimed that the increase in nanofluid viscosity caused enhanced production due to field orientation and the creation of large chains of nanoparticles. Pourafshari and Alfarsi (2019) argued that the nanoparticles might increase water thermal conductivity, energy absorption, and consequently, the oil production. Therefore, they utilized gamma-alumina (γ -Al₂O₃) nanoparticles at a concentration of 0.15 wt% and reported an oil recovery of 40.5% within 1000 W power and 2450 MHz frequency. Al Farsi et al. (2016) used two gamma-alumina and TiO₂ nanoparticles to investigate thermal conductivity, emulsion viscosity, and oil production at a frequency of 2.45 GHz and a power of 1000 W. The results revealed that lower concentrations of TiO₂ (0.05 wt%) had higher thermal conductivity, but gamma-alumina shows an increasing trend until an optimum concentration of 0.5 wt%. In comparison with TiO₂, gamma-alumina reduced emulsion viscosity more at an optimum concentration of 0.5 wt%. The best Production efficiency of 40% and 42% were reported for the concentration of 0.1 wt% gamma alumina and 0.05 wt% TiO₂, respectively. This can be justified by the difference in the specific surface area of the two nanoparticles.

Although reducing oil viscosity is one of the most affecting factors upon oil recovery, microscopic mechanisms including wettability, adsorption of nanoparticles, and surface properties of the rock must not be overlooked. Wettability also alters the capillary pressure, saturation, and also the tension between rock surface and nanoparticles through affecting the surface loads of the rock. By altering these parameters, the fluid distribution in the porous medium, the amount of irreducible water and also the residual oil will change altogether which consequently will affect the oil production figures (Ahmed and McKinney, 2011). Wettability depends on several factors such as oil composition and amount of asphaltene, type of rock and its surface charges, temperature and pressure, the geometry of the pore space, composition of water, salinity, and pH (Ahmed and McKinney, 2011; Taheri-Shakib et al., 2018b). Modifying each of the mentioned factors may change the oil contact angle with the rock surface and thus might significantly impact on the oil production. As the wettability of the rock shifts towards the hydrophilic, capillary pressure decreases and spontaneous imbibition occurs which therefore causes the imbibition of wetting fluid into the porous media. Moreover, the oil phase is detached from the rock surface, and water will be substituted by taking its place. As a result, the oil displacement will become much more efficient. Despite all the efforts carried out, the simultaneous effect of electromagnetic waves and nanoparticles on rock and fluid properties is still vague and untouched. Regarding the electromagnetic radiation on colloidal fluids such as nanofluids, in addition to increasing the fluid temperature, the Brownian motion of the particles also changes (Liboff, 1966). Furthermore, due to the electromagnetic field alternative direction, charged and magnetic particles are oriented in that direction. As the particles move, the colloidal stability and disjoining pressure will change, and the amount of nanoparticles adsorbed on the rock surface will vary.

Also, the temperature affects the adsorption capacity of the rock depending on whether the adsorption of nanoparticles is endothermic or exothermic (Ahmadi and Shadizadeh, 2018). Previous studies have merely investigated the simultaneous effects of nanoparticles and electromagnetic waves macroscopically. The microscopic effects of this hybrid process, such as nanoparticle stability and rock wettability alteration under electromagnetic waves have not been comprehensively focused.

Therefore, in this study, nanoparticles of Fe_3O_4 and $\text{TiO}_2/\text{Fe}_3\text{O}_4$ are first synthesized by the co-precipitation method. Thereafter, for the purpose of stability in water, these nanoparticles as well as commercial TiO_2 nanoparticles have been modified by citric acid. The temperature rise and stability of these nanoparticles under the irradiation were also measured. Then, after the microwave irradiation at 2450 MHz and power levels of 50% and 100%, the wettability alteration of the carbonate rock is measured in the presence of TiO_2 , Fe_3O_4 and $\text{TiO}_2/\text{Fe}_3\text{O}_4$ nanoparticles. Consequently, the amount of oil outflow from the rock is obtained by measuring the weight changes of the rock and will be compared with other results. Furthermore, inductively coupled plasma (ICP) and pH tests have been measured to obtain the ion displacement and its effect on the fluid. On the other hand, according to the above, there is the question of how will the waves affect the absorption of nanoparticles on the rock surface. To answer such question, the adsorption rate of nanoparticles after radiation has been measured at the optimal concentration. Another contributory factor that affects the oil production, as well as wettability, is the oil viscosity. Accordingly, the oil viscosity after microwave radiation has been measured in two modes of with and without the presence of nanoparticles.

2. Materials and method

2.1. Rock and fluids

The carbonate rock sample with 97% of calcium carbonate has a porosity of 38%. For the wettability test, the rock sample is cut into thin sections with a diameter of 38.1 mm and a thickness of 2 mm. The oil sample taken from one of the Iranian oil fields has an API gravity of 15° and a viscosity of 481 cP at room temperature. Three types of nanoparticles, iron oxide (Fe_3O_4), titanium dioxide (TiO_2), and $\text{TiO}_2/\text{Fe}_3\text{O}_4$ composites were utilized in this study. It should be noted that TiO_2 was purchased from the US nano Research Company and the two remaining nanoparticles were synthesized in the laboratory.

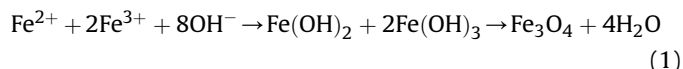
In the synthesis of nanoparticles, deionized water has been used for the purpose of washing. Also, $\text{FeCl}_3 \cdot 6\text{H}_2\text{O}$ and $\text{FeCl}_2 \cdot 4\text{H}_2\text{O}$ has been employed as precursors for the synthesis of Fe_3O_4 . Moreover, ammonia (25 vol%) has been utilized to increase the pH of the solution and prevent precipitation of precursors. Moreover, citric acid has been applied to modify the surface of nanoparticles, and ultimately, nitrogen gas was used to deoxygenate the environment.

2.2. Synthesis of the nanoparticles

2.2.1. Fe_3O_4

Any high temperature calcination converts Fe_3O_4 to γ or α - Fe_2O_3 (Gharibshahi et al., 2020). For this reason, co-precipitation method is commonly used to synthesize nanoparticles without any calcination process. It must be considered that co-precipitation method is one of the oldest methods of synthesizing nanoparticles and it is also used to synthesize Fe_3O_4 nanoparticles. The advantage of this method is that it is an inexpensive and time-saving one. Large amounts of nanoparticles can also be synthesized at low reaction volumes (Nawaz et al., 2019). In this method, Fe^{2+} and Fe^{3+} ions

precipitate in the presence of OH^- through the following reaction (Nawaz et al., 2019):



The system illustrated in Fig. 1 is used to synthesize Fe_3O_4 nanoparticles. To synthesize this substance, 1.72 g of $\text{FeCl}_2 \cdot 4\text{H}_2\text{O}$ and 4.67 g of $\text{FeCl}_3 \cdot 6\text{H}_2\text{O}$ are added to a three-neck flask containing 200 mL of water and stirred vigorously for 10 min. The flask is located in a water bath at 80 °C. Thereafter, while the solution is being stirred vigorously, the ammonia (25 vol%) is added to the solution in a dropwise way for 15 min. During such process, the pH of the solution is measured. The final pH obtained is 11. After this step, the solution is then stirred for another 30 min for better uniformity and distribution of the particles throughout the solution. Finally, the resulting solution is washed several times with deionized water and separated by 0.4 T magnet which results in the entire separation of nanoparticles. The separated particles are dried at 60 °C in a vacuumed condition and stored in powder form. It should be noted that nitrogen gas has been used to remove oxygen from the environment and thus prevent the occurrence of any unwanted reactions including the conversion of Fe_3O_4 to Fe_2O_3 .

2.2.2. $\text{TiO}_2/\text{Fe}_3\text{O}_4$

To synthesize the nanocomposite, 2 g of purchased TiO_2 is first added to 200 mL of water and sonicated for 30 min. The colloidal solution is then placed in the previous system and stirred vigorously. Like the Fe_3O_4 synthesis, iron oxide precursors are first added and stirred for 5 min in the presence of nitrogen gas at 80 °C. It must be regarded that the next steps are like the previous section. Regarding this nanocomposite, the amounts of the two materials are equal, and the magnetic properties of the nanocomposite increase as the TiO_2 quantity decreases (Liu et al., 2012).

2.3. Surface modification

The nanoparticles used in this study are not stable in the aqueous environment by themselves, and this instability initiates many errors in the results. For the stability of these nanoparticles, it is necessary to change the surface charge of these materials and increase the so-called zeta potential. In this study, citric acid, which

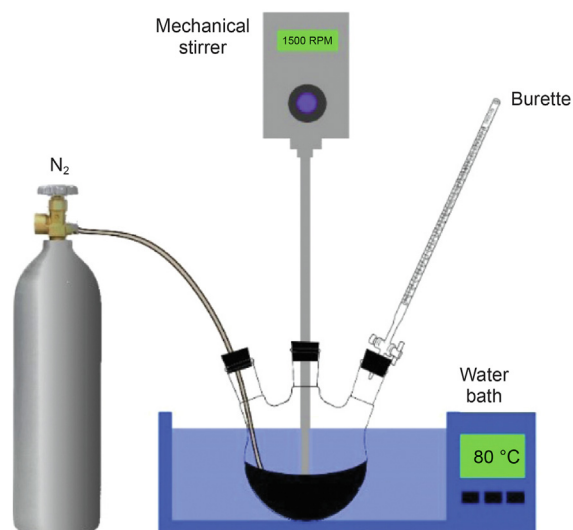


Fig. 1. Nanoparticle synthesis and modification setup.

is highly soluble and stable in water, was used to coat surfaces of nanoparticles. The surface modification of Fe_3O_4 and $\text{TiO}_2/\text{Fe}_3\text{O}_4$ nanoparticles has been performed similarly (Sabzi dizajyekan et al., 2019). A dispersion is prepared from 2 g of citric acid and 4 mL of water and placed inside the ultrasonic bath for better dissolving. In the synthesis stage, after washing the nanoparticles, they are returned to the three-neck flask in the water bath and stirred by a mechanical mixer. The citric acid solution is then added to the flask drop by drop for 2 h. However, the reaction medium is vigorously stirred. After finishing the work, the obtained nanofluid is washed several times with deionized water and kept as a solution. Surface modification of TiO_2 is as follows:

First, a solution with a certain concentration of TiO_2 nanoparticles is prepared and placed in an ultrasonic bath for 30 min. Thereafter, 18 μL of hydrochloric acid is added to the solution until the pH of the solution reaches less than 3 and it is stirred in a water bath at 85 °C for half an hour. Then 2 g of citric acid is dissolved in 4 mL of deionized water and is then added in a dropwise way to the solution from the previous steps and is stirred vigorously for 2 h. The solution is rinsed several times with deionized water until the pH of the solution reaches above 5. Ultimately, the solid particles are separated from the solution by centrifugation and placed in an oven at 60 °C for 12 h.

2.4. Characterization techniques

FTIR analysis (PerkinElmer Spectrum Version 10.03.06) was used to check the existing bonds of the synthesized nanoparticles. The X-ray diagram of the nanoparticles was obtained by a X'Pert MPD of the Philips Company using Co Anode (1.78901 Å). By applying Scherrer's formula and the X-ray line-broadening technique, the average crystalline size of the nanopowder was then measured. The particles morphology was observed by field emission scanning electron microscopy (FESEM) (FEI ESEM Quanta 200). Furthermore, in order to evaluate magnetic properties of nanoparticles, vibrating sample magnetometry (VSM) with a maximum magnetic field of 10 kOe was used at room temperature.

2.5. Experimental setup for static tests

To compare the effect of different nanofluids on rock wettability, it is mandatory that some parameters including the nanoparticle concentration be equal in the all cases compared. Due to the sharp rise in temperature during the irradiation process, the water contained in the nanofluid evaporates and the concentration of nanofluid changes. To do this, a system, as shown in Fig. 2, is designed and a condenser is installed in it. The condenser prevents water to evaporate and therefore the fluid concentration remains relatively unchanged.

In these methods, the test rock is surrounded by nanofluid and after a while, the rock is separated from the nanofluid and its contact angle is measured by the sessile drop method. Considering the radiation, due to the fact that the reaction speed is very high, the irradiation time is greatly reduced. According to the pre-tests, three times of 6, 28 and 55 min have been selected. The time of 6 min is based on the fact that no changes has been observed in the contact angle of oil with the rock. Also, after 55 min, the performance of the microwave oven sharply drops and the obtained data proves to be significantly scattered. Also, the time of 28 min falls between the other two times.

As depicted in Fig. 2, the prepared rock and fluids are placed in a cylindrical container and then connected to a condenser by a converter. Finally, the whole system is placed inside the microwave. In this system, the condenser condenses the evaporated fluid and reverts it to the container. Microwave with a frequency of

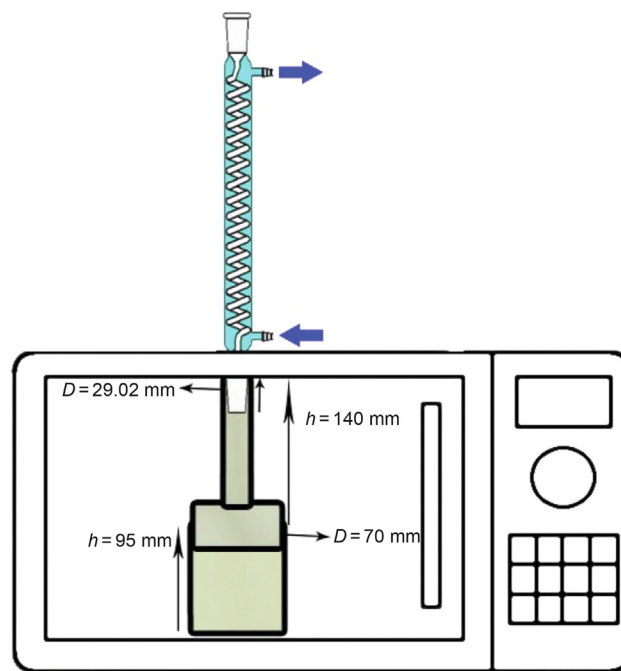


Fig. 2. Designed setup for static tests.

2450 MHz and power levels of 100% and 50% were used to irradiate the samples. The Mastech Model M56531C infrared thermometer was employed to measure the temperature changes of the microwave-irradiated fluids.

2.6. Wettability measurement

In this study, the sessile drop method was used to measure the wettability of the rock. For this purpose, an oil droplet is placed on the rock surface. Preliminary experiments show that after 10 min of dropping a drop of oil on the rock, the oil contact angle with the rock does not change and the so-called oil reaches equilibrium. Therefore, this time is the basis of contact angle tests. After 10 min, when the droplet is in equilibrium with the rock, the photos are taken. The left and right angles of the droplet are measured by Image-J software, and the mean angles are reported. Also, The ICP and pH tests are taken from the optimal samples to understand the governing mechanisms. The procedure for performing the wettability test is as follows:

- The nanoparticles are dispersed in water through sonicating the whole colloids for half an hour.
- Initial contact angle of the oil with the rock is measured in the presence of deionized water.
- Firstly, a thin section of the rock is placed in 25 mL of prepared nanofluid for 48 h without irradiation, and then oil contact angle with the rock is measured (Moslan et al., 2016).
- After that, 25 mL of nanofluid with a thin section of rock is inserted into the designed setup and irradiated at two power levels of 50% and 100%; and at three irradiation times of 6, 28, and 55 min. It should be noted that this method is new and does not exist in the literature and the authors came up with the idea to do this research.
- When the irradiation is over, the rock is separated from the solution and it is set aside for one day to reach equilibrium. Consequently, the oil contact angle with the rock is measured in the presence of deionized water.

2.7. Imbibition test

As the capillary pressure changes, the external fluid (such as water or nanofluid) penetrates into the rock, and the imbibition phenomenon occurs. In the spontaneous imbibition phenomenon, the nanofluid penetrates into the porous medium (due to surface tension difference) and displaces the oil. Moreover, with increasing temperature due to radiation, the relative permeability to the fluids (both nanofluid and oil) increases (Sola et al., 2007). To calculate the oil outflow, the rock weight is measured once before the test and once after the test. The following equation is used to calculate the oil recovery:

$$R = \frac{m_{oe}}{m_{oi}} = \frac{m_{ri} - m_{ra}}{V_r \phi \rho_o} \times 100\% \quad (2)$$

where R is the oil recovery, %; m_{oe} is the weight of oil extracted, m_{oi} is the initial weight of oil within the rock, m_{ri} is the weight of the rock before the test, m_{ra} is the weight of the rock after the test, V_r is the volume of rock, ϕ is the porosity, and ρ_o is the density of the oil before irradiation.

2.8. Adsorption test

To understand how the waves affect the nanoparticle-rock interaction, the concentration of the nanoparticles that has the best wettability alteration is utilized to measure the adsorption of the nanoparticles. First, three concentrations of 0.05 wt%, 0.1 wt%, and 0.2 wt% were prepared from each nanoparticle, and then the calibration curve was plotted using UV spectrophotometry. Then, according to literature (Monfared et al., 2015; Ahmadi and Shadizadeh, 2013a) 1 g of carbonate rock powder with a size of 200–300 μm is poured into 10 mL of nanofluid solution. This compound is then irradiated at a 50% power level at the best time of the wettability alteration test. Also, for comparison, the rock is exposed to different nanofluids at a concentration of 0.2 wt% without radiation for 24 h. After the test is completed, the rock powder is removed from the solution using a 200- μm mesh. Finally, UV absorbance (UV spectrophotometry) of this solution is measured, and the calibration chart reads its concentration. The absorption of the nanoparticles is obtained from the difference between the primary concentration and after irradiation concentrations obtained from the calibration curve.

2.9. Viscosity measurement

Oil viscosity is one of the characteristics that is highly dependent on temperature. This feature is also one of the main and determining parameters in the amount of oil production. As the temperature changes, the viscosity of the oil also changes, and typically, at low pressures, the viscosity of the oil decreases with increasing temperature (Ahmed and McKinney, 2011). The temperature of the oil increases with the radiation of electromagnetic waves, and consequently, its viscosity changes depending on the type of oil (Shang et al., 2018). To achieve a clear understanding of the mechanisms governing the process, oil viscosity has been measured under the following conditions.

A certain amount of oil is inserted into the system, and its viscosity is measured by the AntonPar CD Rheometer. Initially, to determine the effect of temperature on oil viscosity, 30 mL of oil is placed in the rheometer, and its viscosity is measured at a temperature range of 20–80 $^{\circ}\text{C}$. To obtain the effect of the microwave on the oil viscosity, the oil is irradiated at different times with a time increment of 5 min, and after the oil has been cooled for 4 h, its viscosity is measured. To investigate the effect of nanoparticles on

oil viscosity after radiation, the optimal concentration of each nanoparticle is combined with oil and stirred for half an hour. The resulting oil is irradiated at the optimal time obtained in the previous stages, and after the oil cools, its viscosity is measured at ambient temperature.

3. Results and discussion

3.1. Characterization of nanoparticles

Fig. 3 illustrates the result of FTIR test of TiO_2 , Fe_3O_4 and $\text{TiO}_2/\text{Fe}_3\text{O}_4$ nanoparticles in the range of 4000–400 cm^{-1} . Peaks 1636 cm^{-1} and 3370 cm^{-1} represent the hydroxyl group of water adsorbed on the surface of nanoparticles, which are specific to the curvature of the H–O–H bond and the tensile vibration of the H–O, respectively. Also, the peak at 1039 cm^{-1} and 1340 cm^{-1} may be due to the vibration of Ti–O and Fe–O–Ti bonds (Khashan et al., 2017; Salamat et al., 2017). The range 700–400 cm^{-1} corresponds to the vibration of the Ti–O–Ti and Fe–O bonds of the $\text{TiO}_2/\text{Fe}_3\text{O}_4$ composite nanoparticles (He et al., 2008), with a peak of 592 cm^{-1} for the Fe–O tensile vibration (Khashan et al., 2017). Peaks 690 cm^{-1} and 784 cm^{-1} are specific to the vibrations of Ti–O (Al-Amin et al., 2016) and Ti–O–Ti (Salamat et al., 2017), which are greatly reduced according to the intensity chart of these peaks. This decrease is due to radiation absorption by Fe_3O_4 nanoparticles. The overlap of the Ti–O and Fe–O peaks during this period caused it to widen, indicating that the Fe_3O_4 nanoparticles adhered to the TiO_2 surface and were successfully synthesized. The peaks obtained from this study are compared with previous studies and are listed in Table 1.

Fig. 4 demonstrates the XRD analysis of the synthesized $\text{TiO}_2/\text{Fe}_3\text{O}_4$ nanoparticles measured by a cobalt tube made by Philips' X'Pert MPD from the Netherlands. According to the specified peaks, two substances, Fe_3O_4 and TiO_2 , have been detected. The peaks of 35.31 $^{\circ}$, 41.57 $^{\circ}$, 43.2 $^{\circ}$, 50.69 $^{\circ}$, 62.8 $^{\circ}$, 67.47 $^{\circ}$, 74.2 $^{\circ}$ indicate the peaks specific to Fe_3O_4 crystal (JCPDS card No. 19–629) (Khashan et al., 2017). These sharp peaks indicate good crystallization of magnetite particles with the typical inverted cubic spinel structure. Also, the peaks of 29.67 $^{\circ}$, 44.45 $^{\circ}$, 56.63 $^{\circ}$, 63.85 $^{\circ}$, 65.25 $^{\circ}$, 74.45 $^{\circ}$, 82.07 $^{\circ}$, 84.17 $^{\circ}$ are for TiO_2 anatase with tetragonal crystal structure (Horn et al., 1972). According to the shape, Fe_3O_4 peaks are stronger than TiO_2 peaks, indicating that Fe_3O_4 nanoparticles adhere to TiO_2 (Salamat et al., 2017). Also, due to the fact that the TiO_2 in the synthesized nanocomposite ($\text{TiO}_2/\text{Fe}_3\text{O}_4$) has weaker peaks than the pure TiO_2 nanoparticles, it can be concluded that the synthesized nanocomposite is in the core/shell structure. The absence of other peaks confirms the absence of other phases, and no chemical

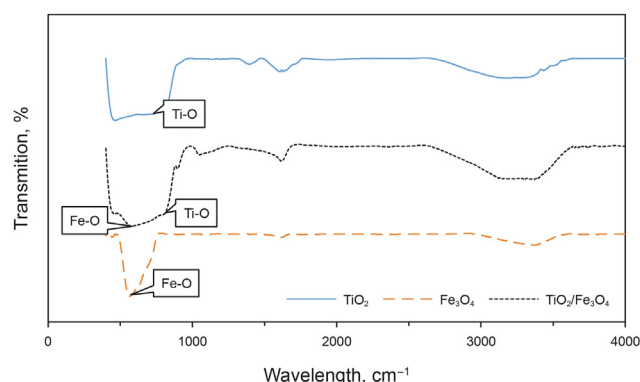


Fig. 3. FTIR comparison of TiO_2 , Fe_3O_4 and $\text{TiO}_2/\text{Fe}_3\text{O}_4$.

Table 1
Adsorption index peak of functional groups present in TiO₂/Fe₃O₄ nanocomposite.

Functional group	Absorption index peak, cm ⁻¹	Reference
Fe–O	592	(Salamat et al., 2017; Khashan et al., 2017)
Ti–O	690	(Salamat et al., 2017; Khashan et al., 2017)
Ti–O–Ti	784	Khashan et al. (2017)
Ti–O	1039	Al-Amin et al. (2016)
H–O–H	1636	Khashan et al. (2017)
O–H	3122–3370	Salamat et al. (2017)

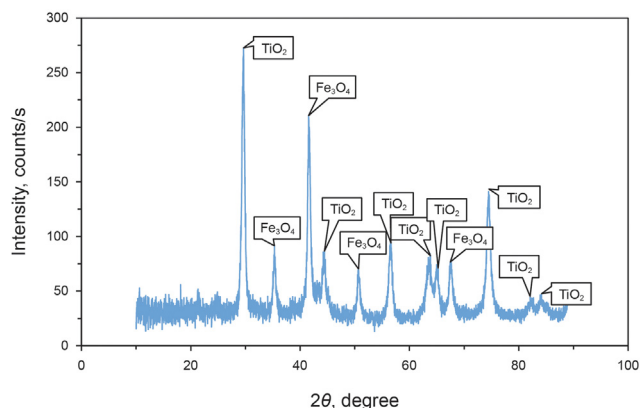


Fig. 4. X-ray diffraction pattern of the synthesized TiO₂/Fe₃O₄.

reaction has occurred between TiO₂ and Fe₃O₄, and the adhesion of the two nanoparticles is solely due to the presence of adhesion forces. In addition to the X-ray diffraction test, the black color as well as the high magnetic strength of the nanoparticles (Fig. 6) confirm the formation of magnetite on the TiO₂ crystals. The crystal size of the synthesized nanoparticles was calculated using the Scherer formula (Salamat et al., 2017; Omidi et al., 2020):

$$D_p = \frac{K\lambda}{B\cos\theta} \quad (3)$$

where D_p is the crystal size, λ is the wavelength equal to 1.54178 Å for the cobalt tube, B is the FWHM XRD peak, and θ is the XRD peak position. The average nanoparticle crystal size is calculated to be 20.23 nm. According to Fig. 5, which shows the FESEM image of nanoparticles, it can be observed that the synthesized

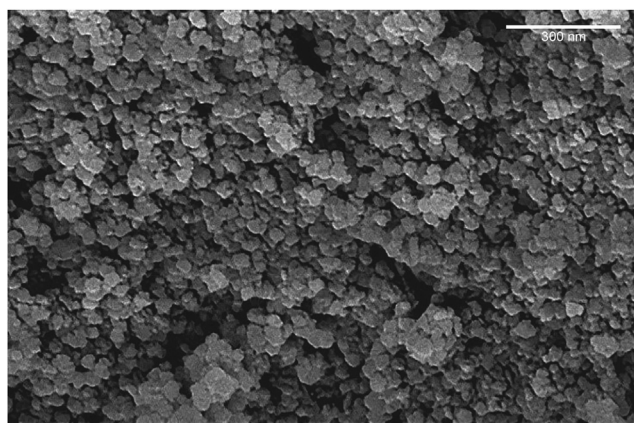


Fig. 5. Field scanning electron microscopy (FESEM) image of TiO₂/Fe₃O₄ nanoparticles at a magnification of 240,000 times.

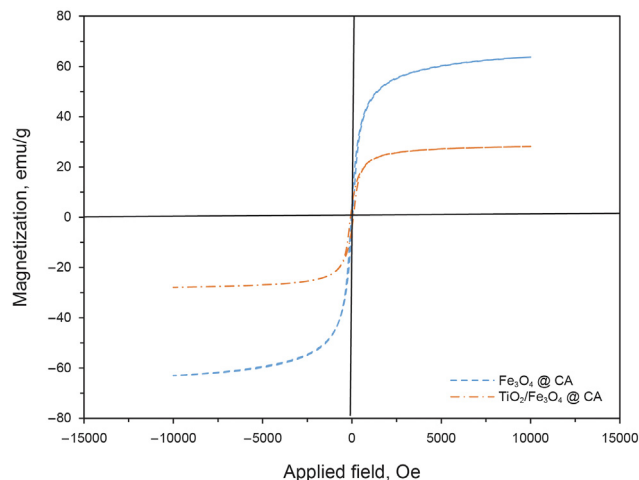


Fig. 6. VSM analysis of Fe₃O₄ and TiO₂/Fe₃O₄ nanoparticles.

nanoparticles have a spherical structure and a particle size of 15–40 nm. The magnetic property of this material causes the particles to stick to each other or to clump. Drying the suspended particles in the liquid also causes them to clump, and the large size of these nanoparticles might prove this fact.

Fig. 6 shows the magnetization properties of Fe₃O₄ nanoparticles and TiO₂/Fe₃O₄ nanocomposite after the surface modification. According to Fig. 6, the magnetic saturation of these two nanoparticles is 63.74 and 28 emu/g, respectively. Therefore, in comparison with bare Fe₃O₄ with magnetic saturation of 93 emu/g (Iida et al., 2007), it can be noted that TiO₂, and citric acid, have a significant adverse impact on the magnetic property of Fe₃O₄. Modification of the surface with citric acid creates a thick layer with very weak magnetic properties on the surface of nanoparticles. Although citric acid increases the stability of the nanofluid, it reduces the bipolar interaction between the particles, an important parameter in Néel relaxation theory, and the dissipation efficiency, which in turn reduces the wave absorption rate (de Sousa et al., 2013). It is worthy to note that the results in this section are consistent with previous studies (Sabzi dizajyekan et al., 2019; Liu et al., 2012). The diagram is S-shape like and no hysteresis loop is observed, indicating superparamagnetic behavior.

TiO₂ has a dielectric constant of 86 and no magnetic properties (Reddy et al., 2003). When electromagnetic waves are emitted, TiO₂ absorbs the electric field of the waves and generates heat as it polarizes. Synthesis of TiO₂/Fe₃O₄ nanoparticles alters the properties of each of the TiO₂ and Fe₃O₄ nanoparticles. Thus, the features of these nanoparticles are a combination of the properties of each of the nanoparticles mentioned. TiO₂ does not merely exhibit magnetic properties, but as previously mentioned, synthesized nanocomposite has a magnetic saturation of 28 emu/g. This is much less than the magnetic saturation of Fe₃O₄, which has a value of 63 emu/g. Also, its dielectric properties are lower than TiO₂ and higher

than Fe₃O₄. These nanoparticles are then expected to produce results similar to or between two other nanoparticles.

3.2. Stability of nanoparticles under irradiation

The stability of the nanoparticles or, in general, a colloidal solution depends on the electrostatic forces between the particles. The higher the repulsive force than van der Waals, the greater the tendency of the nanoparticles to repel each other, so the more stable the solution will be. Nanoparticles such as Fe₃O₄ and TiO₂ are unstable in water and precipitate after a short time. Nanoparticle instability reduces their performance in the interaction between rock and fluid. Surface modification techniques are used to increase stability. In which hydrophilic materials are used and coated on the surface of the nanoparticles. The mechanism of the surface modifiers is that the electrostatic forces between the colloidal particles increase, and thus the stability is increased. The zeta potential for the three Fe₃O₄, TiO₂, and TiO₂/Fe₃O₄ nanoparticles are illustrates in Table 2. Since the absolute magnitude of the zeta potential is greater than 30 mV, thus the nanoparticles are stable (Sun et al., 2016).

In addition to quantitative stability, qualitative stability was also investigated. According to the observations, the synthesized nanocomposite has no precipitation up to three days. On the third day, the upper part of the solution becomes clearer, indicating a low deposition of nanoparticles. TiO₂ nanoparticles become unstable after 8 h, and Fe₃O₄ nanoparticles after one month have neither precipitated nor discolored.

To investigate the effect of microwave on nanoparticle stability, the nanofluid is first placed into the microwave at power level of 50% and irradiated for 1 min. No instability was observed in the synthesized nanocomposites (TiO₂/Fe₃O₄) and also Fe₃O₄ nanoparticles. According to zeta potential data (Table 2), only TiO₂ is unstable under irradiation and Table 3 proves precipitation of TiO₂ nanoparticles. TiO₂ has no magnetic properties and has poor orientation in the electromagnetic field. Accordingly, TiO₂ becomes unstable and precipitates merely by increasing temperature due to radiation. It can be said that with radiation, materials that absorb more energy and are more dynamic in the presence of electromagnetic waves are more stable, and hence the negative effect of increasing temperature is eliminated. It must be mentioned that with increasing temperature, the probability of collision and clumping of nanoparticles increases. In addition, the faster change of direction creates long chains of nanoparticles and thus the nanofluid viscosity increases (Alnarabiji et al., 2018).

3.3. Effect of nanoparticles on electromagnetic heating efficiency







Different nanoparticles have different dielectric properties and subsequently absorb different microwave energy. Fig. 7 shows the temperature changes versus irradiation time for different fluids including deionized water, TiO₂, Fe₃O₄, and TiO₂/Fe₃O₄ water-based nanofluids at microwave levels of 100% and 50%.

Continuous radiation, which is the result of the microwave power level of 100%, causes the temperature to rise more than other power levels. Among these nanoparticles, Fe₃O₄ is most capable of

Table 2
Zeta potential of nanoparticles.

Nanoparticle type	Zeta potential, mV	
	Before irradiation	After irradiation
TiO ₂	-30	-12
Fe ₃ O ₄	-89	-81
TiO ₂ /Fe ₃ O ₄	-48	-35

Table 3
Qualitative analysis of nanoparticle stability after 1 min of microwave irradiation at power level of 50%.

Nanoparticle type	Before irradiation	After 1 min irradiation
Fe ₃ O ₄		
TiO ₂ /Fe ₃ O ₄		
TiO ₂		

absorbing waves and converting them to heat energy. Both TiO₂/Fe₃O₄ and TiO₂ have approximately equal temperature gradient at lower power.

Fe₃O₄ has the highest magnetic saturation. This means that in the electromagnetic field, it responds faster to the field and stores more energy. TiO₂ does not have magnetic properties, but it has a high dielectric constant (Reddy et al., 2003) and is capable of absorbing microwave oscillating electric field. Therefore, TiO₂ has a higher ability to absorb and convert the energy compared to water. The slower growth of TiO₂ nanofluid temperature than other nanoparticles might be attributed to higher energy gap of the TiO₂ band. TiO₂ has a dielectric constant of 86, non-magnetic properties, and a 3.2 eV energy gap (Reddy et al., 2003), which is a good absorber for the electromagnetic field in the frequency range of 13–18 GHz (Zhu et al., 2010). The microwave used in this study has a frequency of 2.450 GHz. At this frequency, the TiO₂ absorbs microwave less than the higher frequencies. So there is a need for more energy to move electrons from one band to another. This energy is obtained at longer times of radiation.

The temperature difference at a constant time varies for different nanoparticles dissolved in various base fluids. The water begins to evaporate when it reaches a temperature of 100 °C. This phase change in the open environment has little effect on the fluid temperature. Oil has a lower dielectric constant than water (Callarotti and Paez, 2014; Liu et al., 2018). Therefore, it has a slower temperature slope than water. But oil components have a different boiling point and can grow temperatures up to 250 °C or higher at longer irradiation time (Hu et al., 2017).

Fig. 8 also indicates an increase in temperature of the oil containing nanoparticles after 5 min of irradiation. According to Fig. 8, TiO₂ exhibits the lowest temperature increase compared to other nanoparticles, and Fe₃O₄ has the highest temperature increase. The order of power of these particles in increasing the oil temperature is the same as their order in increasing the water temperature.

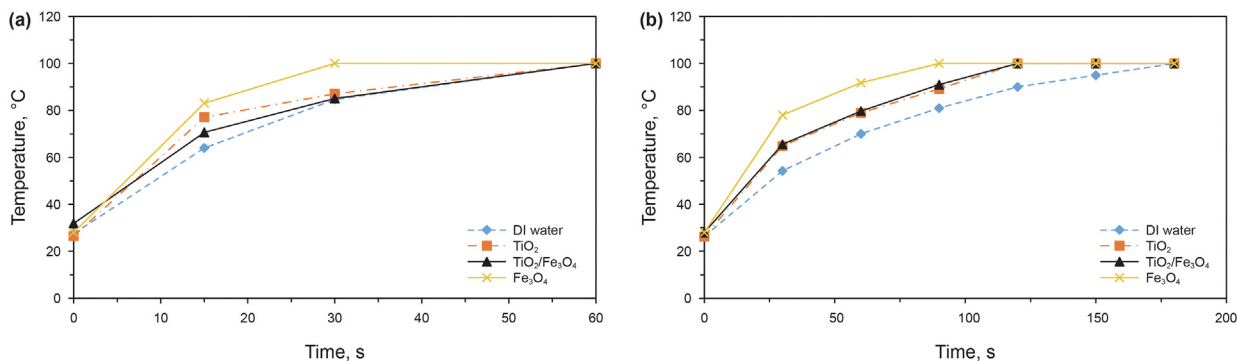


Fig. 7. Temperature changes with time for different fluids at different power levels of (a) 100% and (b) 50%.

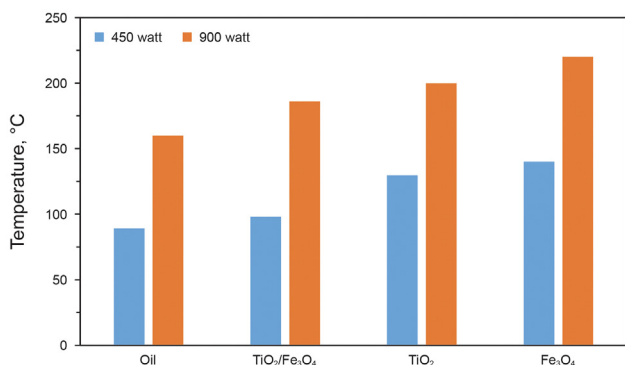


Fig. 8. Increased oil temperature in the presence of nanoparticles after 5 min of microwave irradiation.

3.4. Effect of nanoparticles on rock wettability

Fig. 9 shows rock wettability alteration in the presence of nanoparticles without radiation. According to Fig. 9, $\text{TiO}_2/\text{Fe}_3\text{O}_4$ nanocomposite has the best efficiency in contact angle reduction. Note that the rock was in contact with nanofluids for 48 h.

Contact angle diagram and oil droplet photography for TiO_2 nanofluid are brought in Fig. 10 and Table 4, respectively. It can be perceived from Fig. 10 that 0.05 wt% and 0.1 wt% of TiO_2 nanofluids have little effect on the wettability of rock, but 0.2 wt% TiO_2 nanofluid decreases contact angle from 160° to 30° after 55 min of irradiation. In this section, power levels have ignoring differences. Fig. 11 and Table 5 demonstrate that by utilizing Fe_3O_4 nanofluid at

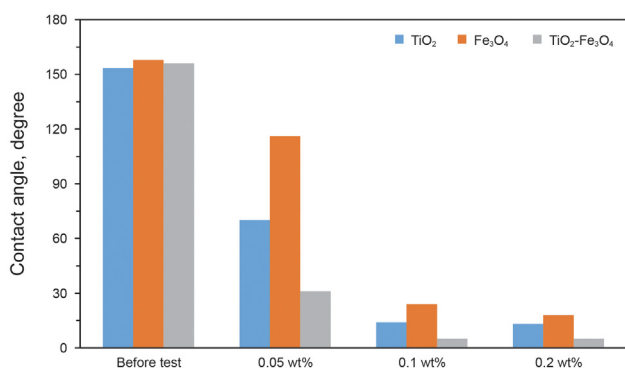


Fig. 9. Rock wettability alteration by different nanofluids at 100 °C without irradiation after 48 h of nanofluid-rock contact.

the optimum time of 28 min, the power level of 50%, and the concentration of 0.2 wt%, it will result the highest drop in contact angle and also the strong hydrophilic angle of 19° .

Unlike TiO_2 at concentrations of 0.05 wt% and 0.1 wt%, Fe_3O_4 has a significant effect on this process, which at a concentration of 0.1 wt% after 55 min of irradiation, the rock exhibits neutral wettability. Fe_3O_4 Concentrations of 0.05 wt% and 0.1 wt% gave almost similar results in the change of wettability at the power level of 50%. This proves that higher concentrations will give better results, but at level of 100%, this difference increases. There is also a significant difference in the power effect as the power level 50% is particularly superior to level 100%.

Unmodified iron oxide (Fe_3O_4) with a magnetic saturation of 80 emu/g (Sabzi dizajyekan et al., 2019) is an excellent absorber for the microwave magnetic field. Wen et al. (2012) showed that in the range of 2.13–6.02 GHz, the magnetic loss is much higher than the dielectric loss, and after that, the dielectric loss increases further.

Fig. 12 and Table 6 show the effect of synthesized $\text{TiO}_2/\text{Fe}_3\text{O}_4$ nanocomposite on the rock wettability under microwave irradiation at two power levels of 50% and 100%. It is worth to note that the initial oil contact angle with rock is 159° and 156° for lower and higher powers, respectively. At 28 min of radiation and 0.2 wt% concentration, the changes in contact angle at 50% and 100% power levels are 71.8% and 51.25%, respectively, confirming the more significant effect of power level of 50% compared to level of 100%.

According to Figs. 10–12, the concentrations of 0.05 wt% and 0.1 wt% in TiO_2 and $\text{TiO}_2/\text{Fe}_3\text{O}_4$ show little effect on the wettability of the rock, but Fe_3O_4 nanoparticles at these concentrations have a significant impact on the contact angle. For example, the concentration of 0.1 wt% of Fe_3O_4 in 55 min increases wettability from strongly oil-wet (151.5°) to neutral (94°). The common point of all graphs is that irradiation time and power, respectively, have a maximum and minimum effect on the oil contact angle. According to Fig. 9, in the absence of microwave radiation, the $\text{TiO}_2/\text{Fe}_3\text{O}_4$ nanocomposite has the best effect on wettability, but in the presence of these waves, it is Fe_3O_4 that reacts better under irradiation. This may be due to the stability, zeta potential, and microwave absorption properties of the nanoparticles.

It must be noted that the wettability depends on the surface charges (Taheri-Shakib et al., 2018b; Chibowski et al., 1994; Buckley et al., 1989). Positive surface charge (calcite or carbonate rock) absorbs negatively charged tail of polar oil components such as carboxylic acid through polar attraction (Mehrabanfar et al., 2021); therefore, these rocks tend to be oil-wet. On the contrary side, negatively charged rocks such as quartz or sandstone tend to repel the oil components and exhibit hydrophilic properties (Ahmadi et al., 2015). Accordingly, an external electric or magnetic field can alter the wettability by disrupting the order of electrical

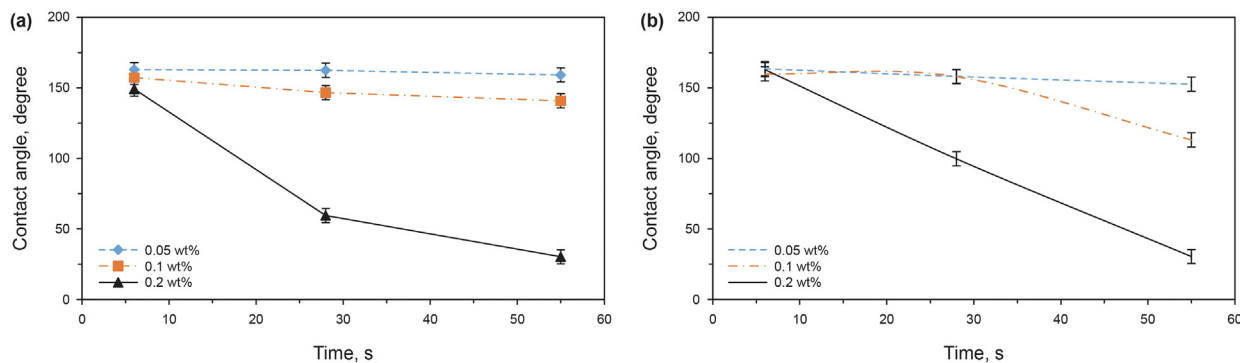


Fig. 10. Oil-rock contact angle changes during irradiation at different concentrations of TiO₂ and different power levels of (a) 50% and (b) 100%.

Table 4

Oil droplet on the rock surface after exposing the rock at different power levels and irradiation time in the presence of TiO₂.

Power level	Time of irradiation, min		
	6	28	55
50%			
100%			

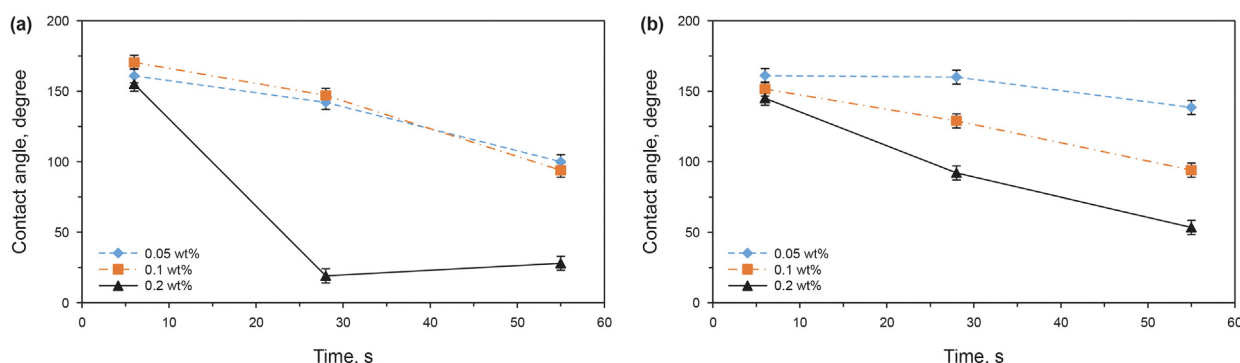


Fig. 11. Oil-rock contact angle changes during irradiation at different concentrations of Fe₃O₄ and different power levels of (a) 50% and (b) 100%.

Table 5

Oil droplet on the rock surface after exposing the rock at different power levels and irradiation time in the presence of Fe₃O₄.

Power level	Time of irradiation, min		
	6	28	55
50%			
100%			

charges. According to Fig. 13, at constant temperature and pressure, the nanoparticles apply a constant pressure (called disjoining pressure) onto an oil drop on a solid surface. By using an oscillating

electric field, the colloidal particles begin to oscillate and produce an acoustic wave due to the electroacoustic phenomenon (Zhang and Austad, 2006). The generated acoustic wave alternately forces

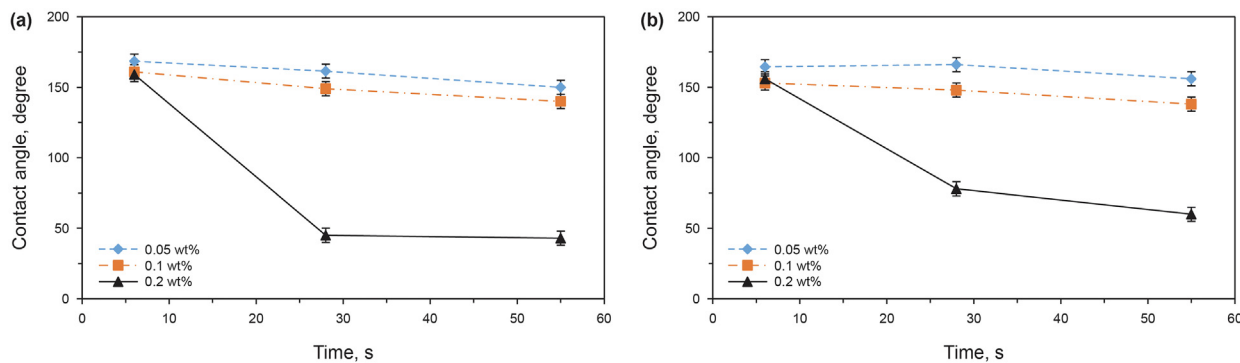


Fig. 12. Oil-rock contact angle changes during irradiation at different concentrations of TiO_2/Fe_3O_4 and different power levels of (a) 50% and (b) 100%.

Table 6

Oil droplet on the rock surface after exposing the rock at different power levels and irradiation time in the presence of TiO_2/Fe_3O_4 .

Power level	Time of irradiation, mins		
	6	28	55
50%			
100%			

the oil absorbed on the rock; therefore, the disjoining pressure changes due to the vibration of ions and particles, the energy loss, and the forces acting on the microwave-affected system. As disjoining pressure increases, the oil phase is extracted from the rock surface with greater efficiency (Wasan et al., 2011), and hydrophilic nanoparticles are adsorbed on the rock surface instead of oil (Abhishek et al., 2019). Adsorption of nanoparticles alters the wettability of the rock to hydrophilic. The higher the magnetic and dielectric properties of the nanoparticles, the better the reaction to electromagnetic waves.

Nanoparticle stability data after irradiation (Tables 2 and 3) also confirms the greater effectiveness of Fe_3O_4 and TiO_2/Fe_3O_4 magnetic nanoparticles than TiO_2 . TiO_2 instability reduces disjoining pressure. It also lowers the absorption of nanoparticles and

precipitates on the walls of rock surfaces.

Fig. 14 shows FESEM images of the rock before and after the radiation. Fig. 14(a) illustrates that after the rock is aged, the oil is well absorbed on the rock surface and into the cavities and forms a complete oil-wet surface. In addition, Fig. 14(b and c) are images of the rock after 28 min of radiation at 0.2 wt% of Fe_3O_4 nanoparticles with power level of 50%. Additionally, from Fig. 14(b) it can be perceived that almost all the oil has been extracted from the rock. As can be seen from Fig. 14(c), Fe_3O_4 nanoparticles are adsorbed on the rock surface, and there are no traces of oil. Because of their magnetic properties, Fe_3O_4 nanoparticles adhere to each other and form larger particles, which is evident in Fig. 14(c) by varying the size of the particles. Fig. 14 (d and e) shows the adsorption of the synthesized nanocomposite and TiO_2 nanoparticles on the rock surface, respectively.

Table 7 lists the adsorption results of nanoparticles, which indicates that microwave has a significant effect on the particle charges and intermolecular forces. Adsorption of the Fe_3O_4 nanoparticles on the surface of the rock is more than other nanoparticles, which is consistent with the mentioned results. Higher adsorption of nanoparticles can cover more area of the rock surface and make the rock surface charges uniform. However, higher adsorption could alter wettability more efficiently, but is not economically viable.

Asphaltene, carboxylic acid, and naphthenic acid are the main constituents of petroleum, which due to their negative charge, are adsorbed on carbonate rock surfaces with a positive charge and are the main factors of rock oil wetness (Taheri-Shakib et al., 2018b). As the system temperature increases, the interfacial tension between the water and the oil decreases (Hamouda and Rezaei Gomari, 2006) as well as the oil density, which reduces the oil contact angle with the rock according to the following formula:

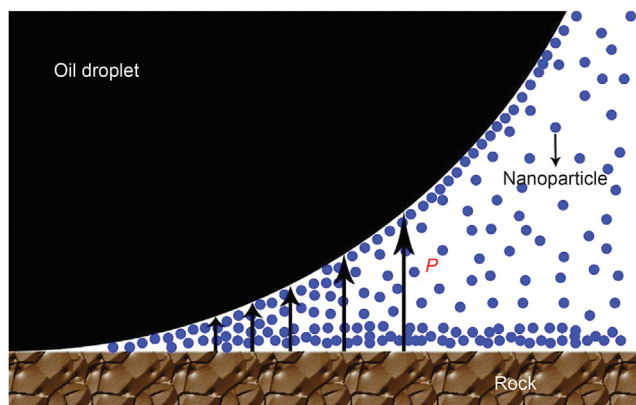


Fig. 13. Schematic view of adsorption of nanoparticles on rock and roll of disjoining pressure.

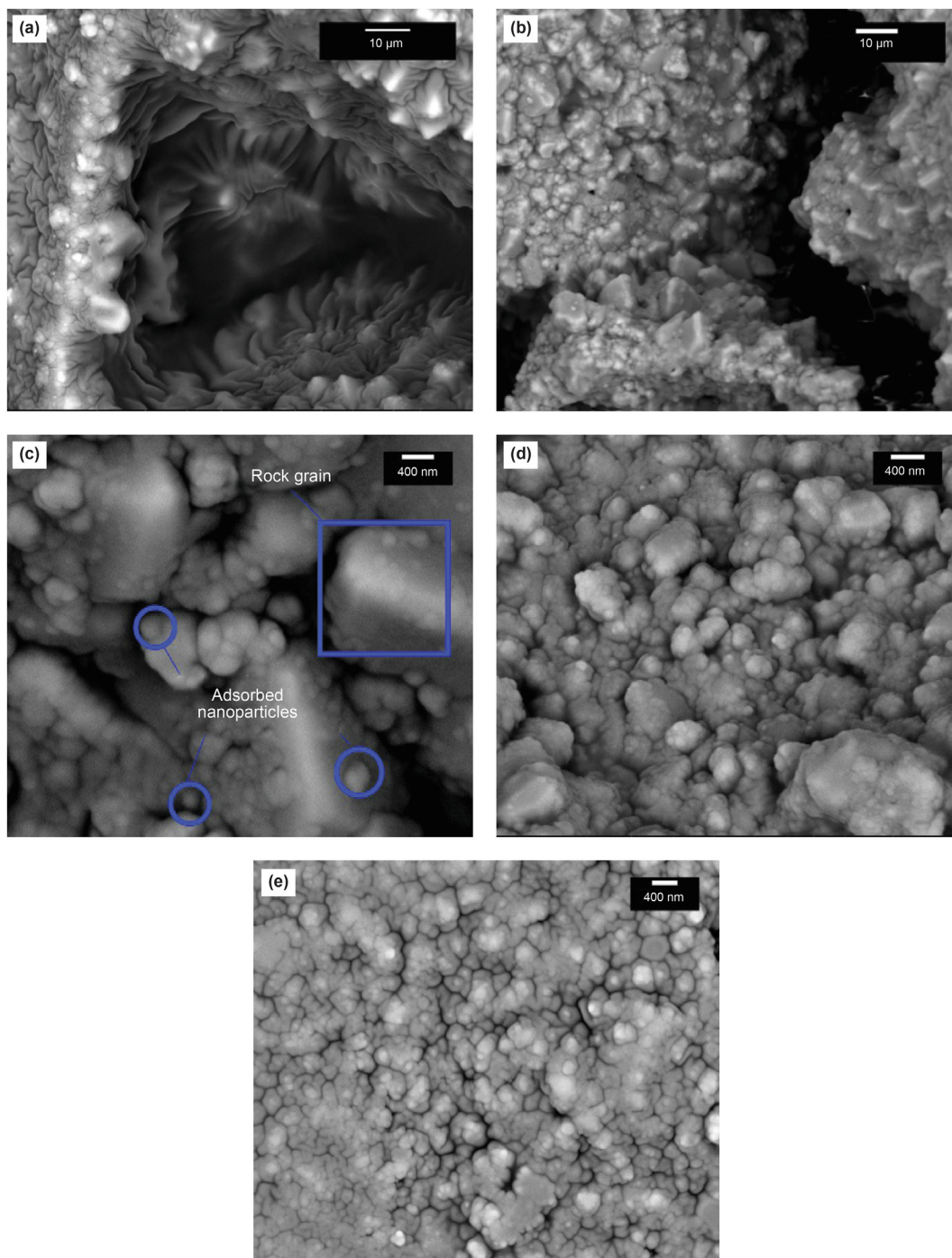


Fig. 14. FESEM images of carbonate rock surface under test: (a) after rock aging and before radiation, (b) after radiation, (c) higher magnification and absorption of Fe₃O₄ nanoparticles, (d) adsorption of TiO₂/Fe₃O₄ nanocomposite, and (e) adsorption of TiO₂ nanoparticles.

Table 7
 Adsorption of the nanoparticles in two modes of radiation and without radiation.

Nanoparticle type	Adsorption after 28 min of irradiation, mg/L	Adsorption after 1 full day without irradiation, mg/L
Fe ₃ O ₄	3.525	1.35
TiO ₂ /Fe ₃ O ₄	2.80	1.08
TiO ₂	2.62	0.81

$$\sigma = \frac{rh(\rho_w - \rho_{nw})g}{2\cos\theta} \quad (4)$$

where σ is the interfacial tension, r is the pore throat radius, h is the height of capillary rise, ρ_w is the wetting phase density, ρ_{nw} is the non-wetting phase density, and g is gravity.

With temperature increase, the zeta potential of carbonate rock decreases from large positive numbers to small positive ones (Hamouda and Rezaei Gomari, 2006). This phenomenon indicates an increase in repulsion forces between acids separated from oil and the rock surface. It also demonstrates that the calcite surface is deficient in calcium ion charge. It can be observed that the surface required for carboxylic acid adsorption is reduced. Thus, the rock hydrophobicity weakens. Also, Hamouda and Karoussi (2008) stated that both the contact angle of oil with calcite surface and oil-water interfacial tension show a decrease with temperature which is in favor of higher oil recovery. Viscous forces are temperature-dependent and therefore the relative permeability changes with temperature. For a high tension system, as the temperature at a constant saturation increases, the relative oil permeability increases and the relative water permeability decreases, so the relative permeability vs. water saturation diagram shifts toward more water saturation values. Therefore, the rock shows the behavior of hydrophilicity (Punase et al., 2014). As the temperature increases, the solubility of asphaltene in the oil increases (Bera and Babadagli, 2015), and the oil becomes a more stable and uniform colloid. In this case, the asphaltene adsorbed on the rock surface is easily removed from the rock surface and dissolved in the oil; as a result, the surface charge of rock changes from negative to positive, and the rock exhibits hydrophilic properties.

Increasing the environment temperature due to microwave radiation has various effects on fluid-rock interactions as well as fluid-fluid interactions. By electromagnetic radiation and by increasing the ambient temperature, the energy produced is absorbed by the molecules, and bypassing through the bonding energy, it breaks the hydrocarbon bonds, which occur in processes such as cracking, desulfurization, and demetalization. In the cracking process, heavy crude oil molecules such as resin and asphaltene are broken down into lighter molecules. The high temperature and breakdown of the asphaltene and resin molecules make the molecules more stable and soluble in oil (Mohammadi et al., 2016; Escrochi et al., 2008). Asphaltene precipitation is delayed by increasing the onset point (Taheri-Shakib et al., 2018a). Asphaltene molecules, one of the factors affecting the oil-wetness of the rock, are therefore easily removed at high temperatures from the rock surface, resulting in a faster rate of wettability change.

3.5. Imbibition test results

Imbibition is the penetration of external fluid into a porous medium by capillary forces. The greater the fluid infiltration, the greater the output or oil production. Fig. 15 shows the results of oil production from the imbibition process at the optimum concentration (0.2 wt%) of nanofluids from wettability test results.

According to Fig. 15, as the power decreases, the production increases. The power level of half or 50% in the microwave is such that the radiation is switched on and off alternately and uniformly. Continuous irradiation with 100% microwave power to the aqueous fluid creates a superheated zone that prevents steam from escaping and increases the internal pressure of the fluid. This increase in pressure also prevents oil from leaking out. But 50% of the power facilitates the exit of water vapor by disconnecting and reconnecting, and the oil comes out at alternating intervals. The highest

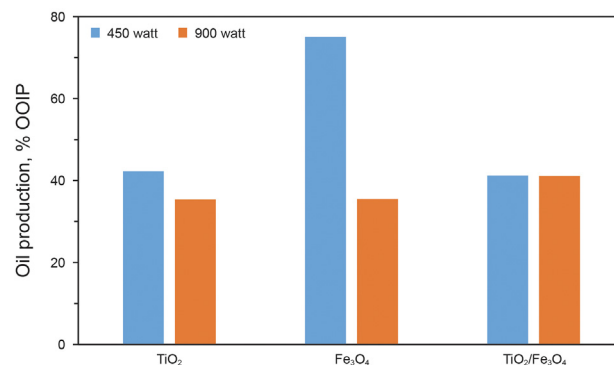


Fig. 15. The rate of oil withdrawal from the irradiated rock during the imbibition process at a concentration of 0.2 wt% and 28 min of irradiation.

oil production is related to Fe₃O₄ nanoparticles, which shows efficiency of approximately 75%. The superiority of Fe₃O₄ nanoparticles can be attributed to the high capacity of this material in absorbing electromagnetic waves based on VSM test data (Fig. 6) and temperature changes (Figs. 7 and 8). The imbibition results are also consistent with the results of the wettability section. The other two nanoparticles show almost equal oil extraction. This efficiency, in a short time, confirms the ability of electromagnetic waves to enhance oil recovery. Fig. 16 shows the oil outflow from the rock surrounded by nanofluid after microwave irradiation. Based on the amount of oil spread on the vessel wall and the effect of water vapor condensate, it can be understood that at the power level of 50%, oil leaves the rock slowly during radiation, but at the power level of 100%, oil leaves the rock in the final stages of radiation.

3.6. Effect of microwave on pH and adsorption of nanoparticles

The acidic and basic properties of the environment depend on the presence of hydroxide ion (OH⁻) and proton ion (H⁺). With increasing proton ions in a solution, the fluid becomes more acidic (pH < 7), and in reverse, by increasing hydroxide ion, the

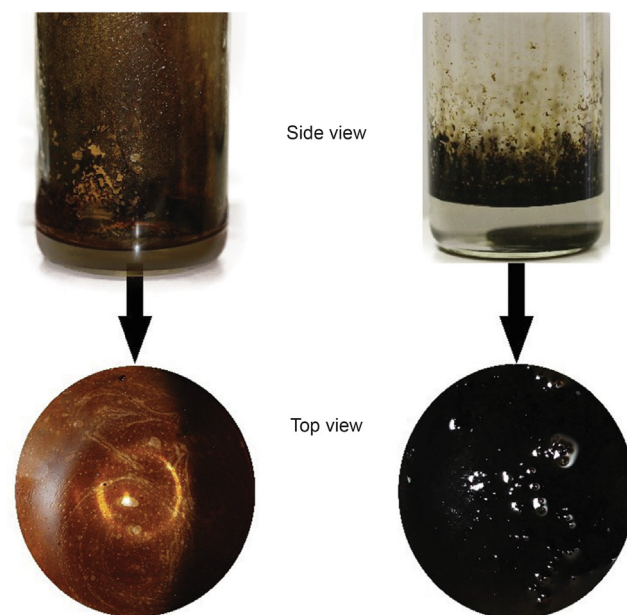
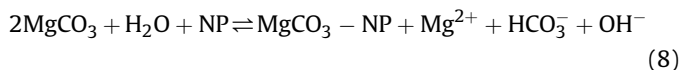
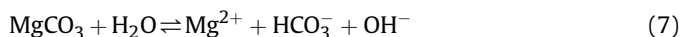
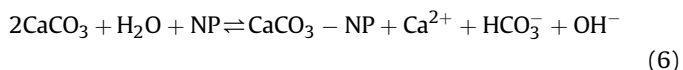
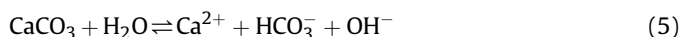


Fig. 16. Oil outflow from the rock after 28 min of irradiation in the presence of TiO₂ and at power levels of 50% (left) and 100% (right).

environment pH shifts towards the basic mode (pH > 7). Fig. 17 elaborates the pH change of nanofluid at a concentration of 0.2 wt % and after 28 min of irradiation at two power levels of 50% and 100%.

Initially, all fluids were acidic. According to Fig. 17, after irradiation, the pH changes from acidic to basic. The pH of TiO₂ varies between 6.0 and 8.7, which is the highest percentage of change among Fe₃O₄ nanoparticles and TiO₂/Fe₃O₄ nanocomposite. At high pH values, carboxylic acid acts like a surfactant which may affect the wettability of the rock (Punase et al., 2014). The mechanism of action of surfactant on wettability exists in several sources in the literature (Ahmadi and Shadizadeh, 2013b, 2017; Ahmadi, 2016).

Depending on the constituents of the rock, two chemical processes may occur between the fluid and the rock. These processes involve dissolving the rock in the fluid and absorbing the nanoparticles on the rock surface (Hamouda and Abhishek, 2019).



Equations (5) and (7) show the dissolution of calcite and magnesium minerals in the water, and Eqs. (6) and (8) show the absorption of nanoparticles on the surface of calcite. In both equations, the release of the hydroxide ion is common, and this ion is the dominant factor in increasing the pH of the medium. Table 8 shows the ICP results of the samples after irradiation.

Table 8 confirms Eqs. (5)–(8). The table also shows that the presence of Fe₃O₄ nanoparticles caused the further dissolution of the calcium ion in the fluid. As seen in previous results, Fe₃O₄ has a greater effect on wettability and imbibition than other nanoparticles. The ICP test also confirms this. Further dissolution of these particles in the nanofluid cleans the rock surface of the oil and oil-friendly agents. Therefore, more nanoparticles are adsorbed on the rock surface, and the wettability of the rock tends to be more hydrophilic. These results show that the adsorption of Fe₃O₄ on the rock surface is higher than other nanoparticles (Table 7).

According to these results, it can be claimed with certainty that electromagnetic waves affect charged and magnetic particles.

Table 8
Results of rock and fluid ion chromatography after 28 min of irradiation at a power level of 50% and 0.2 wt% concentration.

Nanoparticles type	Ca ²⁺ concentration, mg/L	Mg ²⁺ concentration, mg/L
TiO ₂	43.00	13.31
Fe ₃ O ₄	92.706	19.036
TiO ₂ /Fe ₃ O ₄	48.23	9.54

These waves can control the movement of these particles and affect the physical properties of nanofluids, such as viscosity.

3.7. Effect of microwave on oil viscosity

Fig. 18 shows a decrease in oil viscosity with increasing temperature. At ambient temperature, the oil viscosity is 481 cP, which decreases to 25 cP by increasing the temperature to 80 °C. Fig. 19 shows the changes in oil viscosity under microwave irradiation with a power level of 50% at various times with an interval of 5 min. Fig. 19 depicts that by increasing the irradiation time to 5 min, the oil viscosity decreases, and then with increasing time, the viscosity increases so that the oil viscosity reaches 827 cP in 40 min. Oxygen in the environment and atmospheric pressure can be considered as the reasons for the increase in viscosity over time (Shang et al., 2018). At low pressures, lightweight petroleum components are easily separated, and heavy elements remain. The initial decrease in viscosity can be due to the breakdown of large hydrocarbon chains into smaller and lighter components (Taheri-Shakib et al., 2017). The inverse trend of viscosity diagrams over time indicates the exit of light elements or the formation of large chains and polymerization. This conclusion is consistent with the findings of other researchers (Britten et al., 2005; Gunal and Islam, 2000; Mozafari and Nasri, 2017).

The effect of different nanoparticles on the oil viscosity after 5 min of irradiation is shown in Fig. 20. According to Fig. 20 at both level of 100% and 50%, Fe₃O₄ nanoparticles have the most significant effect on reducing the viscosity of the oil so that its viscosity reaches from 481 to 200 cP at the level of 50%. Other nanoparticles show a decrease in oil viscosity, but their effects are not as much as Fe₃O₄ nanoparticles. Figs. 7 and 8 confirms the superiority of Fe₃O₄ nanoparticles in increasing oil temperature, which is consistent with the viscosity results.

This data suggests that, firstly, the reduction of oil viscosity by different nanoparticles is not the same. Because the type of nanoparticles has an important effect on heating rate and temperature rise. Secondly, because the viscosity change is related to the change in the oil properties, the tendency of the oil to adhere to the rock

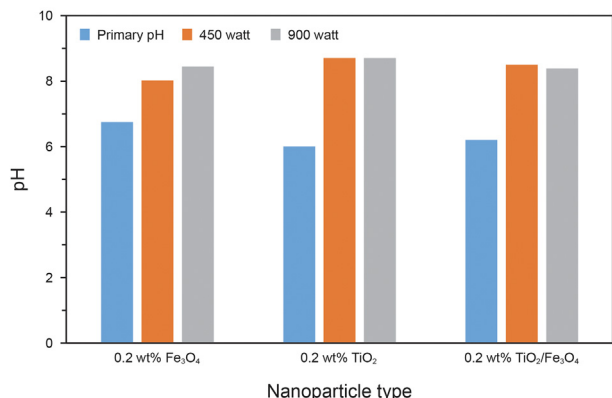


Fig. 17. pH changes of nanofluids after 28 min of radiation at different power levels.

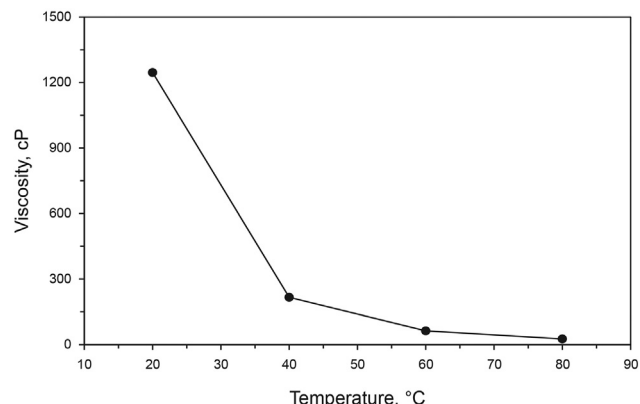


Fig. 18. Viscosity changes versus temperature.

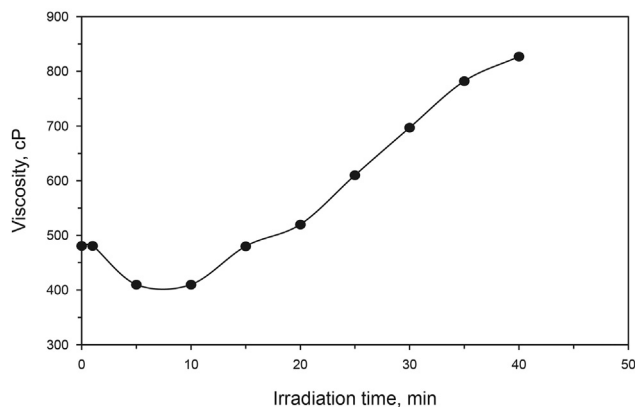


Fig. 19. Oil viscosity changes with irradiation time.

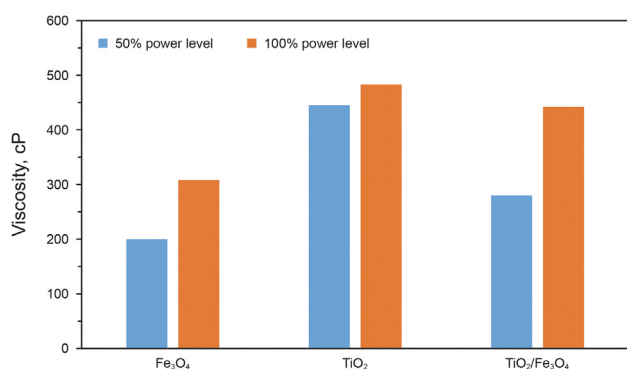


Fig. 20. Effect of different nanoparticles on the oil viscosity at power levels of 100% and 50% and 5 min of irradiation time.

surface changes. To prove this, the oil was irradiated at 5-min intervals, and its viscosity and contact angle with the intact aged rock were measured. Fig. 21 shows a relation between oil-rock contact angle and oil viscosity.

It is clear that with decreasing the viscosity, the contact angle also diminishes, and after increasing the viscosity, the contact angle increases. This indicates that by changing the properties of oil, both physically and chemically, the degree of its tendency to spread on the rock surface also changes. As mentioned earlier, the decrease in the viscosity of the irradiated oil is due to the breakdown of large molecules. Asphaltene is also one of the functional groups that alters the wettability of rocks. As the oil lightens, the amount of asphaltene and, consequently, the tendency of the oil to spread on the rock surface decreases.

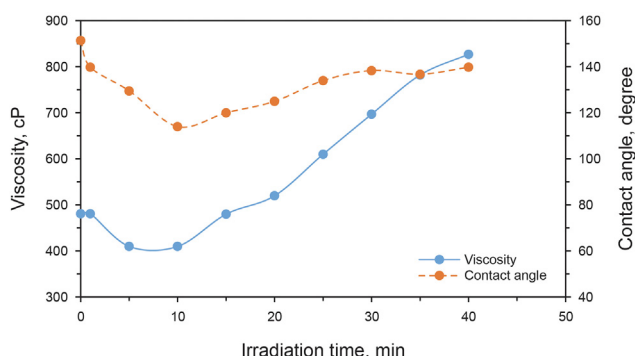


Fig. 21. Oil viscosity change versus oil contact angle with the rock surface.

4. Conclusion

In this research, the effect of three nanoparticles of TiO₂, Fe₃O₄, and TiO₂/Fe₃O₄ nanocomposite on the fluid-rock and fluid-fluid interactions in the presence of microwave radiation has been investigated. TiO₂ nanoparticle is commercially available, but the other mentioned nanoparticles are synthesized by the co-precipitation method. All of the nanoparticles are coated with citric acid for better stability and distribution in water. Identification analysis shows that synthesis and surface modification are successful. The results reveal that the microwave can have excellent efficiency in reducing the contact angle of oil with rock at the optimal power level of 50%. In the presence of Fe₃O₄ nanoparticles, the contact angle is reduced from 155° to 19° in 28 min. During the imbibition process, much oil is produced from the rock in a short period of time. So that 75% of the oil is produced with Fe₃O₄ nanoparticles. According to the additional tests of pH, ICP, and viscosity, it can be concluded that the change in the rock wetness with microwave radiation is affected by various parameters such as oil viscosity and type of nanoparticles. Increasing the temperature dissolves the asphaltene in the oil, reduces the viscosity of the oil, and makes it easier to detach from the rock surface. The disjoining pressure of nanoparticles accelerates the oil detaching process and changes its surface properties by being adsorbed on the rock surface. ICP and pH data indicates the separation and dissolution of calcite in the aqueous medium. As the rock particles are removed, the intact surface of the rock becomes visible and does not contain any oil functional groups.

Overall, the study shows that microwaves increase oil production through various mechanisms such as changing surface charges and rock wettability, reducing oil viscosity, changing the adsorption rate of nanoparticles, and increasing the rock solubility in a fluid. Microwaves have a tremendous ability to change the properties of rock and fluid. They can be used as a clean source of energy to produce oil in the tertiary recovery level or to stimulate oil wells.

Acknowledgments

The authors would like to express their sincere gratitude to the National Iranian South Oil Company (NISOC) for their financial support.

References

- Abhishek, R., Hamouda, A.A., Abdulhameed, F.M., 2019. Adsorption kinetics and enhanced oil recovery by silica nanoparticles in sandstone. *Petrol. Sci. Technol.* 37, 1363–1369. <https://doi.org/10.1080/10916466.2019.1587455>.
- Ahmadi, M.A., 2016. Use of nanoparticles to improve the performance of sodium dodecyl sulfate flooding in a sandstone reservoir. *European Phys. J. Plus* 131, 1–9. <https://doi.org/10.1140/epjp/i2016-16435-5>.
- Ahmadi, M.A., Shadizadeh, S.R., 2013a. Experimental investigation of adsorption of a new nonionic surfactant on carbonate minerals. *Fuel* 104, 462–467. <https://doi.org/10.1016/j.fuel.2012.07.039>.
- Ahmadi, M.A., Shadizadeh, S.R., 2013b. Induced effect of adding nano silica on adsorption of a natural surfactant onto sandstone rock: experimental and theoretical study. *J. Petrol. Sci. Eng.* 112, 239–247. <https://doi.org/10.1016/j.petrol.2013.11.010>.
- Ahmadi, M.A., Shadizadeh, S.R., 2017. Nano-surfactant flooding in carbonate reservoirs: a mechanistic study. *The European Physical Journal Plus* 132, 246. <https://doi.org/10.1140/epjp/i2017-11488-6>.
- Ahmadi, M.A., Shadizadeh, S.R., 2018. Spotlight on the new natural surfactant flooding in carbonate rock samples in low salinity condition. *Sci. Rep.* 8, 1–15. <https://doi.org/10.1038/s41598-018-29321-w>.
- Ahmadi, M.A., Galedarzadeh, M., Shadizadeh, S.R., 2015. Wettability alteration in carbonate rocks by implementing new derived natural surfactant: enhanced oil recovery applications. *Transport Porous Media* 106, 645–667. <https://doi.org/10.1007/s11242-014-0418-0>.
- Ahmed, T., McKinney, P., 2011. *Advanced Reservoir Engineering*. Gulf Professional Publishing. <https://doi.org/10.1016/B978-0-7506-7733-2.X5000-X>.
- Al-Amin, M., Dey, S.C., Rashid, T.U., Ashaduzzaman, M., Shamsuddin, S.M., 2016. Solar assisted photocatalytic degradation of reactive azo dyes in presence of

- anatase titanium dioxide. *International Journal of Latest Research in Engineering and Technology* 2, 14–21.
- Al-Farsi, H., Pourafshary, P., Al-Maamari, R.S., 2016. Application of nanoparticles to improve the performance of microwave assisted gravity drainage (MWAGD) as a thermal oil recovery method. In: SPE EOR Conference at Oil and Gas West Asia. <https://doi.org/10.2118/179764-MS>.
- Alnarabji, M.S., Yahya, N., Nadeem, S., Adil, M., Baig, M.K., Ghanem, O.B., Azizi, K., Ahmed, S., Maulianda, B., Klemes, J.J., 2018. Nanofluid enhanced oil recovery using induced ZnO nanocrystals by electromagnetic energy: viscosity increment. *Fuel* 233, 632–643. <https://doi.org/10.1016/j.fuel.2018.06.068>.
- Anwar, J., Shafiq, U., Rehman, R., Salman, M., Dar, A., Anzano, J.M., Ashraf, U., Ashraf, S., 2015. Microwave chemistry: effect of ions on dielectric heating in microwave ovens. *Arabian Journal of Chemistry* 8, 100–104. <https://doi.org/10.1016/j.arabj.2011.01.014>.
- Archer, D.G., Wang, P., 1990. The dielectric constant of water and Debye-Hückel limiting law slopes. *J. Phys. Chem. Ref. Data* 19, 371–411. <https://doi.org/10.1063/1.555853>.
- Bahraminejad, H., Khaksar Manshad, A., Riazi, M., Ali, J.A., Sajadi, S.M., Keshavarz, A., 2019. CuO/TiO₂/PAM as a novel introduced hybrid agent for water–oil interfacial tension and wettability optimization in chemical enhanced oil recovery. *Energy Fuels* 33, 10547–10560. <https://doi.org/10.1021/acs.energyfuels.9b02109>.
- Bera, A., Babadagli, T., 2015. Status of electromagnetic heating for enhanced heavy oil/bitumen recovery and future prospects: a review. *Appl. Energy* 151, 206–226. <https://doi.org/10.1016/j.apenergy.2015.04.031>.
- Britten, A., Whiffen, V., Miadonye, A., 2005. Heavy petroleum upgrading by microwave irradiation. *WIT Transactions on Modelling and Simulation* 41. <https://doi.org/10.2495/CMEM050101>.
- Buckley, J., Takamura, K., Morrow, N., 1989. Influence of electrical surface charges on the wetting properties of crude oils. *SPE Reservoir Eng.* 4, 332–340. <https://doi.org/10.2118/16964-PA>.
- Callarotti, R., Paez, E., 2014. Microwave dielectric properties of heavy oil and heating of reservoirs. In: SPE Energy Resources Conference, Port of Spain, Trinidad and Tobago. <https://doi.org/10.2118/169937-MS>.
- Chakma, A., Jha, K.N., 1999. Heavy-oil recovery from thin pay zones by electro-magnetic heating. *Energy Sources* 21, 63–73. <https://doi.org/10.2118/24817-MS>.
- Chibowski, E., Hoiysz, L., Wójcik, W., 1994. Changes in zeta potential and surface free energy of calcium carbonate due to exposure to radiofrequency electric field. *Colloid. Surface. Physicochem. Eng. Aspect.* 92, 79–85. [https://doi.org/10.1016/0927-7757\(94\)02949-0](https://doi.org/10.1016/0927-7757(94)02949-0).
- de Sousa, M.E., Fernandez van Raap, M.B., Rivas, P.C., Mendoza Zelis, P., Girardin, P., Pasquevich, G.A., Alessandrini, J.L., Muraca, D., Sánchez, F.H., 2013. Stability and relaxation mechanisms of citric acid coated magnetite nanoparticles for magnetic hyperthermia. *J. Phys. Chem. C* 117, 5436–5445. <https://doi.org/10.1021/jp311556b>.
- Doorwar, S., Mohanty, K.K., 2011. Viscous fingering during non-thermal heavy oil recovery. SPE Annual Technical Conference and Exhibition, Denver, Colorado, USA. doi:10.2118/146841-MS.
- Escrochi, M., Nabipour, M., Ayatollahi, S.S., Mehranbod, N., 2008. Wettability alteration at elevated temperatures: the consequences of asphaltene precipitation. In: SPE International Symposium and Exhibition on Formation Damage Control, February 13–15. <https://doi.org/10.2118/112428-MS>.
- Gharibshahi, R., Omidkhan, M., Jafari, A., Fakhrouiean, Z., 2020. Hybridization of superparamagnetic Fe₃O₄ nanoparticles with MWCNTs and effect of surface modification on electromagnetic heating process efficiency: a microfluidics enhanced oil recovery study. *Fuel* 282, 118603. <https://doi.org/10.1016/j.fuel.2020.118603>.
- Greff, J., Babadagli, T., 2013. Use of nano-metal particles as catalyst under electromagnetic heating for in-situ heavy oil recovery. *J. Petrol. Sci. Eng.* 112, 258–265. <https://doi.org/10.1016/j.petrol.2013.11.012>.
- Gunal, O.G., Islam, M., 2000. Alteration of asphaltic crude rheology with electromagnetic and ultrasonic irradiation. *J. Petrol. Sci. Eng.* 26, 263–272. [https://doi.org/10.1016/S0920-4105\(00\)00040-1](https://doi.org/10.1016/S0920-4105(00)00040-1).
- Hamouda, A.A., Abhishek, R., 2019. Effect of salinity on silica nanoparticle adsorption kinetics and mechanisms for fluid/rock interaction with calcite. *Nanomaterials* 9, 213. <https://doi.org/10.3390/nano9020213>.
- Hamouda, A.A., Karoussi, O., 2008. Effect of temperature, wettability and relative permeability on oil recovery from oil-wet chalk. *Energies* 1, 19–34. <https://doi.org/10.3390/en1010019>.
- Hamouda, A.A., Rezaei Gomari, K.A., 2006. Influence of temperature on wettability alteration of carbonate reservoirs. SPE/DOE Symposium on Improved Oil Recovery, Tulsa, Oklahoma, USA. doi:10.2118/99848-MS.
- He, Q., Zhang, Z., Xiong, J., Xiong, Y., Xiao, H., 2008. A novel biomaterial—Fe₃O₄:TiO₂ core-shell nano particle with magnetic performance and high visible light photocatalytic activity. *Opt. Mater.* 31, 380–384. <https://doi.org/10.1016/j.optmat.2008.05.011>.
- Horn, M., Schwerdtfeger, C.F., Meagher, E.P., 1972. Refinement of the structure of anatase at several temperatures. *Z. für Kristallogr. - Cryst. Mater.* 136, 273. <https://doi.org/10.1524/zkri.1972.136.3-4.273>.
- Hu, L., Li, H.A., Babadagli, T., Ahmadloo, M., 2017. Experimental investigation of combined electromagnetic heating and solvent-assisted gravity drainage for heavy oil recovery. *J. Petrol. Sci. Eng.* 154, 589–601. <https://doi.org/10.1016/j.petrol.2016.10.001>.
- Iida, H., Takayanagi, K., Nakanishi, T., Osaka, T., 2007. Synthesis of Fe₃O₄ nanoparticles with various sizes and magnetic properties by controlled hydrolysis. *J. Colloid Interface Sci.* 314, 274–280. <https://doi.org/10.1016/j.jcis.2007.05.047>.
- Kadeethum, T., Sarma, H., Maini, B., 2017. Overcome viscous fingering effect in heavy oil reservoirs by an optimized smart water injection scheme. In: SPE Canada Heavy Oil Technical Conference. <https://doi.org/10.2118/184966-MS>.
- Khashan, S., Dagher, S., Tit, N., Alazzam, A., Obaidat, I., 2017. Novel method for synthesis of Fe₃O₄@TiO₂ core/shell nanoparticles. *Surf. Coating. Technol.* 322, 92–98. <https://doi.org/10.1016/j.surfcoat.2017.05.045>.
- Liao, H., Morte, M., Bloom, E., Huff, G., Hascakir, B., 2018. Controlling microwave penetration and absorption in heavy oil reservoirs. SPE Western Regional Meeting. <https://doi.org/10.2118/190089-MS>.
- Liboff, R.L., 1966. Brownian motion of charged particles in crossed electric and magnetic fields. *Phys. Rev.* 141, 222. <https://doi.org/10.1103/PhysRev.141.222>.
- Liu, J., Che, R., Chen, H., Zhang, F., Xia, F., Wu, Q., Wang, M., 2012. Microwave absorption enhancement of multifunctional composite microspheres with spinel Fe₃O₄ cores and anatase TiO₂ shells. *Small* 8, 1214–1221. <https://doi.org/10.1002/sml.201102245>.
- Liu, J., Dai, C., Hu, Y., 2018. Aqueous aggregation behavior of citric acid coated magnetite nanoparticles: effects of pH, cations, anions, and humic acid. *Environ. Res.* 161, 49–60. <https://doi.org/10.1016/j.envres.2017.10.045>.
- Mehrabianfar, P., Bahraminejad, H., Manshad, A.K., 2021. An introductory investigation of a polymeric surfactant from a new natural source in chemical enhanced oil recovery (CEOR). *J. Petrol. Sci. Eng.* 198, 108172. <https://doi.org/10.1016/j.petrol.2020.108172>.
- Millemann, R.E., Haynes, R.J., Boggs, T.A., Hildebrand, S.G., 1982. Enhanced oil recovery: environmental issues and state regulatory programs. *Can. J. Chem. Eng.* 7 (3), 165–177. [https://doi.org/10.1016/0160-4120\(82\)90103-9](https://doi.org/10.1016/0160-4120(82)90103-9).
- Mohammadi, S., Rashidi, F., Mousavi-Dehghani, S.A., Ghazanfari, M.H., 2016. On the effect of temperature on precipitation and aggregation of asphaltenes in light live oils. *Can. J. Chem. Eng.* 94, 1820–1829. <https://doi.org/10.1002/cjce.22555>.
- Monfared, A.D., Ghazanfari, M., Jamialahmadi, M., Helalizadeh, A., 2015. Adsorption of silica nanoparticles onto calcite: equilibrium, kinetic, thermodynamic and DLVO analysis. *Chem. Eng. J.* 281, 334–344. <https://doi.org/10.1016/j.cej.2015.06.104>.
- Moslan, M.S., Wan Sulaiman, W.R., Ismail, A.R., Jaafar, M.Z., Ismail, I., 2016. Wettability alteration of dolomite rock using nanofluids for enhanced oil recovery. In: Materials Science Forum. Trans Tech Publ, pp. 194–198. <https://doi.org/10.4028/www.scientific.net/MSF.864.194>.
- Mozafari, M., Nasri, Z., 2017. Operational conditions effects on Iranian heavy oil upgrading using microwave irradiation. *J. Petrol. Sci. Eng.* 151, 40–48. <https://doi.org/10.1016/j.petrol.2017.01.028>.
- Nawaz, S., Sliman, Y., Ercan, I., Lima-Tenório, M.K., Tenório-Neto, E.T., Kaewsaneha, C., Elaissari, A., 2019. Magnetic and pH-responsive magnetic nanocarriers. In: Stimuli Responsive Polymeric Nanocarriers for Drug Delivery Applications. Elsevier, pp. 37–85.
- Omidi, A., Manshad, A.K., Moradi, S., Ali, J.A., Sajadi, S.M., Keshavarz, A., 2020. Smart-and nano-hybrid chemical EOR flooding using Fe₃O₄/eggshell nanocomposites. *J. Mol. Liq.* 316, 113880. <https://doi.org/10.1016/j.jmolliq.2020.113880>.
- Pourafshary, P., Al Farsi, H., 2019. Enhancement of heavy oil recovery by nanoparticle/microwave application. *Eurasian Chemico-Technol. J.* 21, 51–56. <https://doi.org/10.18321/ectj790>.
- Punase, A., Zou, A., Elputranto, R., 2014. How do thermal recovery methods affect wettability alteration? *Journal of Petroleum Engineering.* <https://doi.org/10.1155/2014/538021>.
- Reddy, K.M., Manorama, S.V., Reddy, A.R., 2003. Bandgap studies on anatase titanium dioxide nanoparticles. *Mater. Chem. Phys.* 78, 239–245. [https://doi.org/10.1016/S0254-0584\(02\)00343-7](https://doi.org/10.1016/S0254-0584(02)00343-7).
- Sabzi dizajyekan, B., Jafari, A., Hasani, M., Vafaei-Sefti, M., Fakhrouiean, Z., Baghbansalehi, M., 2019. Surface modification of synthesized Fe₃O₄ superparamagnetic nanoparticles and performance investigation in gelation parameters enhancement: application in enhanced oil recovery. *Appl. Nanosci.* 10, 955–969. <https://doi.org/10.1007/s13204-019-01187-y>.
- Salamat, S., Younesi, H., Bahramifar, N., 2017. Synthesis of magnetic core-shell Fe₃O₄@TiO₂ nanoparticles from electric arc furnace dust for photocatalytic degradation of steel mill wastewater. *RSC Adv.* 7, 19391–19405. <https://doi.org/10.1039/C7RA01238A>.
- Shang, H., Yue, Y., Zhang, J., Wang, J., Shi, Q., Zhang, W., Liu, L., Omar, S., 2018. Effect of microwave irradiation on the viscosity of crude oil: a view at the molecular level. *Fuel Process. Technol.* 170, 44–52. <https://doi.org/10.1016/j.fuproc.2017.10.021>.
- Sola, B.S., Rashidi, F., Babadagli, T., 2007. Temperature effects on the heavy oil/water relative permeabilities of carbonate rocks. *J. Petrol. Sci. Eng.* 59, 27–42. <https://doi.org/10.1016/j.petrol.2007.02.005>.
- Speight, J.G., 2013. Heavy and Extra-heavy Oil Upgrading Technologies. Gulf Professional Publishing.
- Sun, D., Kang, S., Liu, C., Lu, Q., Cui, L., Hu, B., 2016. Effect of zeta potential and particle size on the stability of SiO₂ nanospheres as carrier for ultrasound imaging contrast agents. *Int. J. Electrochem. Sci.* 11, 8520–8529. <https://doi.org/10.20964/2016.10.30>.
- Taheri-Shakib, J., Shekarifard, A., Naderi, H., 2017. The experimental study of effect of microwave heating time on the heavy oil properties: prospects for heavy oil upgrading. *J. Anal. Appl. Pyrol.* 128, 176–186. <https://doi.org/10.1016/j.jaap.2017.10.012>.
- Taheri-Shakib, J., Shekarifard, A., Naderi, H., 2018a. Inhibiting asphaltene precipitation using microwave irradiation: experimental investigation. In: Saint

- Petersburg 2018. <https://doi.org/10.3997/2214-4609.201800144>.
- Taheri-Shakib, J., Shekarifard, A., Naderi, H., 2018b. The study of influence of electromagnetic waves on the wettability alteration of oil-wet calcite: imprints in surface properties. *J. Petrol. Sci. Eng.* 168, 1–7. <https://doi.org/10.1016/j.petrol.2018.04.062>.
- Taheri-Shakib, J., Shekarifard, A., Naderi, H.J.F., 2018c. Heavy crude oil upgrading using nanoparticles by applying electromagnetic technique. *Fuel* 232, 704–711. <https://doi.org/10.1016/j.fuel.2018.06.023>.
- Tunio, S.Q., Tunio, A.H., Ghirano, N.A., El Adawy, Z.M., 2011. Comparison of different enhanced oil recovery techniques for better oil productivity. *International Journal of Applied Science and Technology* 1 (5), 143–153. <https://doi.org/10.1016/j.petrol.2018.04.062>.
- Wasan, D., Nikolov, A., Kondiparty, K., 2011. The wetting and spreading of nanofluids on solids: role of the structural disjoining pressure. *Curr. Opin. Colloid Interface Sci.* 16, 344–349. <https://doi.org/10.1016/j.cocis.2011.02.001>.
- Wen, F., Zhang, F., Zheng, H., 2012. Microwave dielectric and magnetic properties of superparamagnetic 8-nm Fe₃O₄ nanoparticles. *J. Magn. Magn. Mater.* 324, 2471–2475. <https://doi.org/10.1016/j.jmmm.2012.03.013>.
- Zaydullin, R., 2013. Thermal Oil Extraction. Stanford University. <http://large.stanford.edu/courses/2013/ph240/zaydullin1/>.
- Zekri, A.Y., Jerbi, K.K., El-Honi, M., 2000. Economic evaluation of enhanced oil recovery. In: International Oil and Gas Conference and Exhibition in China, Beijing, China. <https://doi.org/10.2118/64727-MS>.
- Zhang, P., Austad, T., 2006. Wettability and oil recovery from carbonates: effects of temperature and potential determining ions. *Colloid. Surface. Physicochem. Eng. Aspect.* 279, 179–187. <https://doi.org/10.1016/j.colsurfa.2006.01.009>.
- Zhu, C.-L., Zhang, M.-L., Qiao, Y.-J., Xiao, G., Zhang, F., Chen, Y.-J., 2010. Fe₃O₄/TiO₂ core/shell nanotubes: synthesis and magnetic and electromagnetic wave absorption characteristics. *J. Phys. Chem. C* 114, 16229–16235. <https://doi.org/10.1021/jp104445m>.